

## From Achiral Porphyrins to Template-Imprinted Chiral Aggregates and Further. Self-Replication of Chiral Memory from Scratch

Rosaria Lauceri,<sup>†</sup> Antonio Raudino,<sup>‡</sup> Luigi Monsù Scolaro,<sup>§</sup> Norberto Micali,<sup>||</sup> and Roberto Purrello<sup>\*,‡</sup>

*Istituto per lo Studio delle Sostanze Naturali di Interesse Alimentare e Chimico Farmaceutico, CNR, Sezione di Catania, Catania, Italy, Dipartimento di Scienze Chimiche, Università di Catania Viale Andrea Doria 6, 95125 Catania, Italy, Dipartimento di Chimica Inorganica, Chimica Analitica e Chimica Fisica, Università di Messina, ICTPN-CNR, Sezione di Messina, Salita Sperone 31, Vill. S. Agata, Messina, Italy, and Istituto di Tecniche Spettroscopiche, ITS-CNR, Messina, Italy*

Received September 25, 2001

Optical activity is commonly related to molecular dissymmetry. Symmetric molecules, however, may also present supramolecular chirality by (i) forming intrinsically chiral assemblies<sup>1a–h</sup> or (ii) aggregating onto chiral polymeric templates (extrinsic chirality).<sup>2a–f</sup> The latter case leads to induced circular dichroism bands (ICD) which, having a conformational origin<sup>2a</sup> (i.e., arising from self-organization of the achiral guest by chiral templates), modify or disappear<sup>2a,c</sup> following matrix conformational transition.

Tunability<sup>3</sup> and memory<sup>2c,4,5</sup> of supramolecular-induced chirality have been already achieved, but no evidence of self-replication of induced chirality has been presented until now.

Chiral systems able to self-replicate in solution are useful in understanding the transfer of information in biologically relevant aggregation processes (i.e., prion-mediated disease, diabetes, etc.), but also for technological applications.

We report evidences that the interaction of opposite-charged, achiral CuT4 and H<sub>2</sub>TPPS (Figure 1) in the presence of chiral aggregates of L- or D-aromatic amino acids leads to a simple but smart chemical system capable of autonomous growth.

Self-aggregation of the above porphyrins in water leads to achiral 1:1 complexes.<sup>6</sup> However, addition of the same porphyrins to aqueous solutions of L- or D-phenylalanine (Phe) at least  $1 \times 10^{-3}$  M leads to mirror images ICD in the Soret<sup>7</sup> region (Figure 2a,b).<sup>8</sup>

According to the ICD conformational origin, monomeric amino acids should not induce chiral aggregates because they generate only locally asymmetric environments. DLS data of the Phe solution (Figure 3) show, indeed, the presence at 30 °C of large Phe aggregates (~60 nm), whose size decreases with increasing temperature, leveling off over 60 °C (~20 nm).<sup>9</sup>

DLS measurements do not give, however, any insight on Phe clusters chirality. Yet, such information can be inferred by using the title assemblies as chirality reporters. Thus, we monitored the ICD of porphyrins added to different amino acid solutions pre-warmed at a given temperature. By increasing the temperature, the ICD decreases paralleling the reduction of Phe mass average molecular weight MW (Figure 3). After 60 °C, the ICD is reduced almost to a noise level suggesting that there are critical cluster sizes and concentrations needed to initiate chiral porphyrin aggregation. Persistence of porphyrin assemblies at high temperature was confirmed by absorption measurements. Therefore, different from

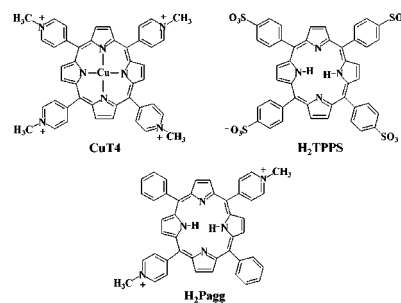


Figure 1. Schematic structures of H<sub>2</sub>TPPS, CuT4 and *t*-H<sub>2</sub>Pagg.

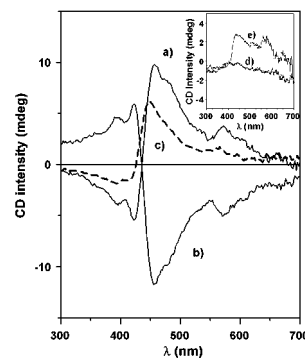


Figure 2. CD spectrum (cuvette path length = 1 cm) of H<sub>2</sub>TPPS and CuT4 ( $2 \times 10^{-6}$  M each) in ultrapure Millipore water in the presence of (a) L-, (b) D-phenylalanine ( $8 \times 10^{-3}$  M), and (c) after the removal of the L-enantiomer. Inset shows the CD spectra of the films of CuT4-H<sub>2</sub>TPPS (d) achiral and (e) imprinted chiral aggregates, respectively.

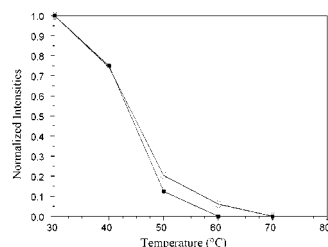


Figure 3. Intensity variations with temperature of ELS of 80 mM L-Phe solutions (circles) and CD in the Soret region of the imprinted CuT4-H<sub>2</sub>TPPS assemblies (squares).

all the previous examples reported in the literature, here the preferential conformation of the porphyrin aggregates is borrowed by *noncovalent* supramolecular chiral templates.

According to our previous results,<sup>2c</sup> the title aggregates are inert enough to memorize the chirality of polymeric templates. A similar

<sup>†</sup> Istituto per lo Studio delle Sostanze Naturali di Interesse Alimentare e Chimico Farmaceutico.

<sup>‡</sup> Università di Catania Viale Andrea Doria 6.

<sup>§</sup> Università di Messina, ICTPN-CNR.

<sup>||</sup> Istituto di Tecniche Spettroscopiche.

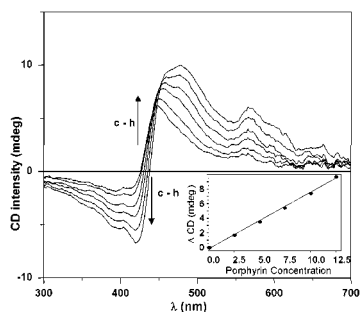


**Figure 4.** CD spectra of the phenylalanine-imprinted aggregates before (c) and after d–h) five additions of the individual porphyrin aliquots ( $2.5 \times 10^{-7}$  M). Inset shows the CD increase ( $\Delta$ CD) vs the added porphyrin concentration ( $M \times 10^7$ ), considering (c) as reference.

result is expected also here after Phe removal.<sup>10</sup> Indeed, ultrafiltration of the solution (Phe residual concentration ca.  $3 \times 10^{-8}$  M)<sup>11</sup> leaves the CD signal almost unaltered (Figure 2c), showing that the imprinted aggregates retain the “memory” of the mold.<sup>12</sup> The inertness of the CuT4–H<sub>2</sub>TPPS aggregates is conceivably related to the synergistic occurrence of an extended network of salt bridges between opposite-charged porphyrins. In fact, the Phe-induced chiral self-assemblies of *t*-H<sub>2</sub>P<sub>agg</sub> (Figure 1), not stabilized by net ionic interactions, do not survive to Phe removal.

SEM data (Supporting Information), obtained by drying the aqueous solutions, allow for direct visualization of the differences between achiral and imprinted chiral porphyrin aggregates. Images of achiral assemblies show an amorphous waxy film whose CD spectrum is featureless as that recorded in aqueous solution (inset of Figure 2, curve d).<sup>13</sup> In contrast, the imprinted chiral aggregates show self-similar structures, and their solid-state CD (inset of Figure 2, curve e) is identical to that obtained in solution.<sup>13</sup>

Different from other examples,<sup>1h,2a,14,15</sup> SEM images do not show evidence of the presence of macroscopic canonical chiral features (helices or twisted ribbons). Yet, theoretical works<sup>16a,b</sup> anticipate that mesoscopic chirality might not be necessarily related to canonical structures, but could derive from intrinsic dissymmetry (e.g., DLA fractals).

The issue is quite intriguing and worth investigating further. If the chirality of the porphyrin complex is expressed to a supramolecular level, the growth process would lead to the growth of the existing chiral species. The scenario that opens foresees the possibility of indefinitely building in solution exact copies of an initial molecule. Indeed, Figure 4 shows that when equimolar amounts of CuT4 and H<sub>2</sub>TPPS are individually added to solutions containing about  $6 \times 10^{-13}$  M of imprinted assemblies (each of them formed by about  $2 \times 10^6$  porphyrin molecules),<sup>17</sup> the ICD of the imprinted aggregates increases and doubles with doubling porphyrins concentration (inset of Figure 4). Interestingly, the linear increase of the CD with porphyrin concentration shows that the chiral growth process is substantially 100% enantiospecific.

Our results unambiguously show that ca.  $10^{-13}$  M<sup>9</sup> of chiral Phe clusters play an initiation role by inducing the formation of similar concentrations of chiral porphyrin assemblies. Thereafter, self-propagation begins. Altogether our data show evidence of a correlated sequence of induction, memory, and amplification of chirality in mesoscopic assemblies. These phenomena involve only noncovalent interactions between polyanions and polycations; however, their synergism gives rise to interactions which are by no means weak. The strength of these forces is the key factor for the memory and propagation of the chiral structures.

The simplicity of this mixing and shaking synthetic approach, the robustness, and the remarkable ability to build exact duplicates

of themselves candidate these imprinted noncovalent aggregates for a wide range of possible technological applications as enantioselective catalysts, racemate resolution agents, and remarkably sensitive *amplifiers* of chirality. Their ability to self-propagate the induced chirality can be seen as a kind of nonenzymatic polymerase chain reaction (PCR) system for amplifying femtomoles of chiral assemblies in water.

**Acknowledgment.** We thank Drs. M. Triscari and G. Sabatino (University of Messina) for SEM measurements and Dr. A. Loisi. This work is partially supported by CNR and MURST.

**Supporting Information Available:** SEM images and elastic light scattering (ELS) data of the achiral and chiral porphyrin aggregates (PDF). This material is available free of charge via the Internet at <http://pubs.acs.org>.

## References

- (1) (a) Kondeputi, D. K.; Kaufman, R. J.; Singh, N. *Science* **1990**, *250*, 975–980. (b) Seto, C. T.; Whitesides, G. M. *J. Am. Chem. Soc.* **1993**, *115*, 905–916. (c) De Rossi, U.; Dähne, S.; Meskers, S. C. J.; Dekkers, H. O. J. M. *Angew. Chem., Int. Ed. Engl.* **1996**, *35*, 760–763. (d) Ferrarini, A.; Moro, G. J.; Nordio, P. L. *Mol. Phys.* **1996**, *87*, 495–499. (e) Atwood, J. L.; MacGillivray, L. R. *Nature* **1997**, *389*, 469–472. (f) Saurez, M.; Branda, N.; Lehn, J.-M.; De Cian, A.; Fischer, J. *Helv. Chim. Acta* **1998**, *81*, 1–13. (g) Rowan, A.; Nolte, R. J. M. *Angew. Chem., Int. Ed.* **1998**, *37*, 63–68. (h) Ribò, J. M.; Crusats, J.; Sagues, F.; Claret, J.; Rubires, R. *Science* **2001**, *292*, 2063–2065.
- (2) (a) Stryer, L.; Blout, E. R. *J. Am. Chem. Soc.* **1961**, *83*, 1411–1418. (b) Gibbs, E. J.; Tinoco, I.; Maestre, M. F.; Ellinas, P. A.; Pasternack, R. F. *Biochem. Biophys. Res. Commun.* **1988**, *157*, 350–358. (c) Pasternack, R. F.; Giannetto, A.; Pagano, P.; Gibbs, E. J. *J. Am. Chem. Soc.* **1991**, *113*, 3, 7799–7800. (d) Purrello, R.; Monsù Scolaro, L.; Bellacchio, E.; Gurrieri, S.; Romeo, A. *Inorg. Chem.* **1998**, *37*, 3647–3648. (e) Bellacchio, E.; Lauceri, R.; Monsù Scolaro, L.; Romeo, A.; Purrello, R. *J. Am. Chem. Soc.* **1998**, *120*, 12353–12354. (f) Purrello, R.; Raudino, A.; Monsù Scolaro, L.; Loisi, A.; Bellacchio, E.; Lauceri, R. *J. Phys. Chem.* **2000**, *104*, 10900–10908.
- (3) Oda, R.; Huc, I.; Schmutz, M.; Candau, S. J.; MacKintosh, F. C. *Nature* **1999**, *399*, 566–569.
- (4) Yashima, E.; Maeda, K.; Okamoto, Y. *Nature* **1999**, *399*, 449–481.
- (5) Prins, L. J.; De Jong, F.; Timmermann, P.; Reinhoudt, D. N. *Nature* **2000**, *408*, 181–183.
- (6) Lauceri, R.; Gurrieri, S.; Bellacchio, E.; Contino, A.; Monsù Scolaro, L.; Romeo, A.; Toscano, A. *Supramol. Chem.* **2000**, *12*, 193–201.
- (7) The Soret band is the main feature in the visible region of the absorption spectrum. Porphyrin assembly is reported in the absorption spectrum as broadening and hypochromicity of this band.
- (8) The same behavior is observed for tryptophan and tyrosine, but the threshold concentration to observe the CD is different for the three amino acids, being ca.  $1 \times 10^{-4}$  M for tyrosine and tryptophane. This trend parallels the amino acids solubility. The porphyrin aggregate solution does not show any linear dichroism signal.
- (9) Figure 3 shows the quantity  $I_{\text{exc}} = I_{\text{sample}} - I_{\text{solvent}}$ , the excess intensity of the scattered light at a right angle. The knowledge of  $I_{\text{exc}}$ , together with that of the hydrodynamic radii (determined by DLS), allowed us to estimate the mass fraction of Phe molecules in the aggregated form to be about  $10^{-5}$  and the cluster molecular weight to be about  $10^8$  Da. Therefore, the concentration of aggregated Phe is  $10^{-7}$  M, and the cluster concentration is  $10^{-13}$  M.
- (10) Phe was removed from the solution by ultrafiltration, using Centricon filters (cutoff = 10 kDa), and the residual concentration was monitored by fluorescence using a Jasco FP-777. The amino acid concentration was checked also in the filtrate. The lower detection limit for Phe is  $\sim 1 \times 10^{-8}$  M. After the disappearance of the Phe emission, three or four further ultrafiltration steps were performed.
- (11) This concentration is far below the threshold to observe the ICD. In this condition, the equilibrium  $n\text{Phe} \rightleftharpoons (\text{Phe})_n$  can be considered as completely shifted toward the monomeric form.
- (12) The imprinted species CD signal remains almost identical up to 85 °C and decreases after 24 h by 40% and 60% in 0.5 and 1 M sodium chloride, respectively. The chiral memory lasts over months even when a strong excess of D-Phe is added to the L-imprinted species (and vice versa).
- (13) Feasibility of solid-state CD has been reported. Kuroda, R. In *Circular Dichroism. Principles and Applications*, 2nd ed.; Berova, N., Nakanishi, K., Woody, R. W., Eds.; Wiley-VCH: New York, 2000; pp 159–184.
- (14) Fuhrhop, J.-H.; Helfrich, W. *Chem. Rev.* **1993**, *93*, 1565–1583.
- (15) Schnur, J. M. *Science* **1993**, *262*, 1669–1676.
- (16) (a) Katzenelson, O.; Zbrodsky Hel-Or, H.; Avnir, D. *Chem.-Eur. J.* **1996**, *2*, 174–182. (b) Katzenelson, O.; Avnir, D. *Chem.-Eur. J.* **2000**, *6*, 1346–1354.
- (17) DLS shows that both chiral and achiral H<sub>2</sub>TPPS–CuT4 aggregates are quite large, the number of involved monomers being ca.  $2 \times 10^6$ .

JA017159B